

**ANALYSIS OF THE DRAINAGE PATTERN IN THE AREA  
AROUND AT'TAIF (KINGDOM OF SAUDI ARABIA)  
BY THE USE OF REMOTE SENSING**

**Asem Y. Bokhari**

*Associate Professor, Faculty of Earth Sciences  
King Abdulaziz University  
P.O. Box 1744, Jeddah 21441  
Saudi Arabia*

الخلاصة :

تمَّ رسم خريطة لنظام الصرف المائي حول مدينة الطائف بالملكة العربية السعودية باستخدام صور القمر الصناعي (لاندسات) ، والبيانات المستخلصة منها وبمعاونة التصوير الجوي . وقد استُخدمت البيانات أيضاً في رسم كلِّ من الحدود الفاصلة بين التكوينات الصخرية المختلفة والخطوط البنيوية المتعددة مثل الشقوق والصدوع وغيرها . كما أُجريت دراسات حقلية لتحقيق النتائج التي تمَّ التوصل إليها عن طريق الاستشعار عن بُعد وجمع عينات مائية للتحليل الكيميائي . وأمكن تأكيد النموذج البنيوي المقترح للمنطقة — موضوع الدراسة — باستخدام الطرق الاحصائية المساندة بالحاسوب . وتوضَّح هذه الدراسة العلاقات بين نموذج الصرف المائي والوضع الجيولوجي والبنيوي للمنطقة المدروسة ، كما تؤكد على الإمكانيات الهائلة التي تتيحها بيانات الاستشعار عن بُعد في المجالات التي تحتاج إلى تداخل العديد من التخصصات .

**ABSTRACT**

Using both the LANDSAT-Thematic Mapper data and aerial photography, the drainage system of the area around the Saudi Arabian city of At'Taif was mapped.

The satellite data served also to delineate both the lithological boundaries and the tectonic elements, such as, fractures, faults, and other lineaments.

A ground survey was carried out to verify the results obtained.

The outline of the structural model for the investigated area was supported by statistical, computer-assisted methods.

The study emphasizes the close relationship between the drainage pattern and the geologic set-up of the region as well as the fact that remote sensing can also contribute to a better understanding of large areas with numerous multidisciplinary problems.

## ANALYSIS OF THE DRAINAGE PATTERN IN THE AREA AROUND AT'TAIF (KINGDOM OF SAUDI ARABIA) BY THE USE OF REMOTE SENSING

### 1. INTRODUCTION

The overall climate of Saudi Arabia falls within Thornthwaite's [1, 2] arid province. Perennial rivers do not exist and the wadi systems have water only for a very short time after heavy rain showers. This water runs off, percolates or evaporates rapidly. Permanent water shortage and scarce vegetation have set tight limits and influenced development in that vast arid land [3].

Recently the Kingdom has witnessed great developments. These were achieved through development plans with increasing emphasis on regional development [4].

Such significant changes have resulted in increasing demands on the water resources of the Kingdom. This has necessitated the preparation of a national water plan involving multidisciplinary investigations, (such as, hydrological data collection and analysis, an inventory of surface and groundwater resources, *etc.*) [5]. The water shortage is mostly felt in the Western Region which contains four large cities of the Kingdom namely, Makkah, Jeddah, Madinah, and At'Taif [6]. A wide range of projects were undertaken to explore the water resources of Saudi Arabia [7].

### 2. THE STUDY AREA

The study area (Figure 1) is part of the Hijaz Mountain Range which is largely composed of eroded and dissected rocks of Precambrian ages, extending from the Gulf of Aqaba to the southern regions of Yemen. The most prominent geomorphologic feature is the tectonically controlled escarpment which lies to the west of the city of At'Taif, and rises to more than 2000 m elevation.

Because of its position near the escarpment towards the Red Sea, the At'Taif area, receives relatively more frequent and abundant rainfalls as expressed by the average level of 162.4 mm/annum (measurement cycle 1962–1972) [7]. However, these favorable climatic conditions are insignificant compared to the water needs of the area, particularly as the rainfalls are irregular. The predominance of the outcropping crystalline rocks minimize infiltration, and the high relief energy causes high runoff rates. The construction of dams which was extensively used in the past, cannot be the final solution today.

Within the framework of a multidisciplinary project, remote sensing data have been recently used for the evaluation of the water resources of the western region of Saudi Arabia (including the At'Taif region).

### 3. DATA PROCESSING AND ANALYSIS

For the current project, the LANDSAT-Thematic Mapper TM (Figure 2a) scene path 169, row 43 acquisition data March 1987, ID. No. 5111407050x0 were purchased. Images collected in Spring are optimum for applications in Saudi Arabia as the vegetation is at its best and the atmosphere is rather clear during this season. The data were recorded in quarter scenes at 6.250 bpi density. Furthermore, they were geometrically corrected, rectified, adjusted and presented in a basically distortion free Universal Transverse Mercator projection (UTM). This projection is also corrected for earth rotation effects. Moreover, 200 aerial photographs (taken in 1956) at an approximate scale of 1:60 000 were used for the mapping task.

For the differentiation of geologic units, from the TM data bands, those which correlate least, *i.e.* bands 1, 4, and the Short Wave Infrared band 7, were registered and processed in several sequential steps to achieve a maximum differentiability [8].

In order to exploit fully the spectral, spatial, and temporal contents of the data, digital image processing was found necessary. The subject of image processing is far too large to be treated here [9] but details have been previously described by Bokhari [10, 11].

Nevertheless, it may help to review briefly the adopted procedure which proved to yield the best results. The image processing procedure implies:

stretching of band 1 (range 104–215), band 4 (range 43–145) and band 7 (range 47–185) to full range;

transformation of the stretched bands to the intensity, hue, and saturation (IHS) color space;

50% dodging of intensity beginning at gray level 175, fixed hue, and raising the saturation component by 90 gray values;

contrast enhancement using an add-back high filter;

retransformation to RGB with a simultaneous stretch of green (levels 0–26) to full range;

generation of a visual display of the processed satellite data using an optronic photowrite system;

recording and merging black and white extracts corresponding to the colors red, green, and blue *via* a photographic composing process yielding positive color rendition;

scanning the original color transparencies, then splitting the colors as displayed into four colors, yellow, cyan, magenta, and black. A laser drum plotter is used where the four colors were displayed as black and white transparencies in the final scale which serves to produce lithographies *i.e.* the plates for offset printing in the final map scale of 1:50 000 providing the basis for geologic and tectonic interpretation.

From these “lithographic black and white extracts”, yellow and cyan were taken for a second black and white image, which provided the basis for the evaluation of the drainage pattern.

Interpretation of the satellite images, was carried out visually, taking into account existing literature, maps, and the aerial photographs. The latter provided essential information, especially, for mapping the drainage system, due to their high geometric resolution and stereoscopic coverage. Such photographs served for delineating watersheds in coherent valleys, which could not be identified on satellite images. They also helped to determine the run-off direction, to distinguish between the anthropogenous and natural linear elements, and also between outcropping rocks and alluvial sediments. The first draft of interpreting remote sensing data was then controlled and verified along significant profiles [12].

#### 4. GEOLOGIC SETTING OF THE AREA

The geologic setting of the area (Figure 2b) reveals that Cryptozoic rocks are spotted — in places — by basaltic flows of Paleogene to Holocene age.

The Precambrian formations outcropping in the mapped area can be briefly listed as follows:

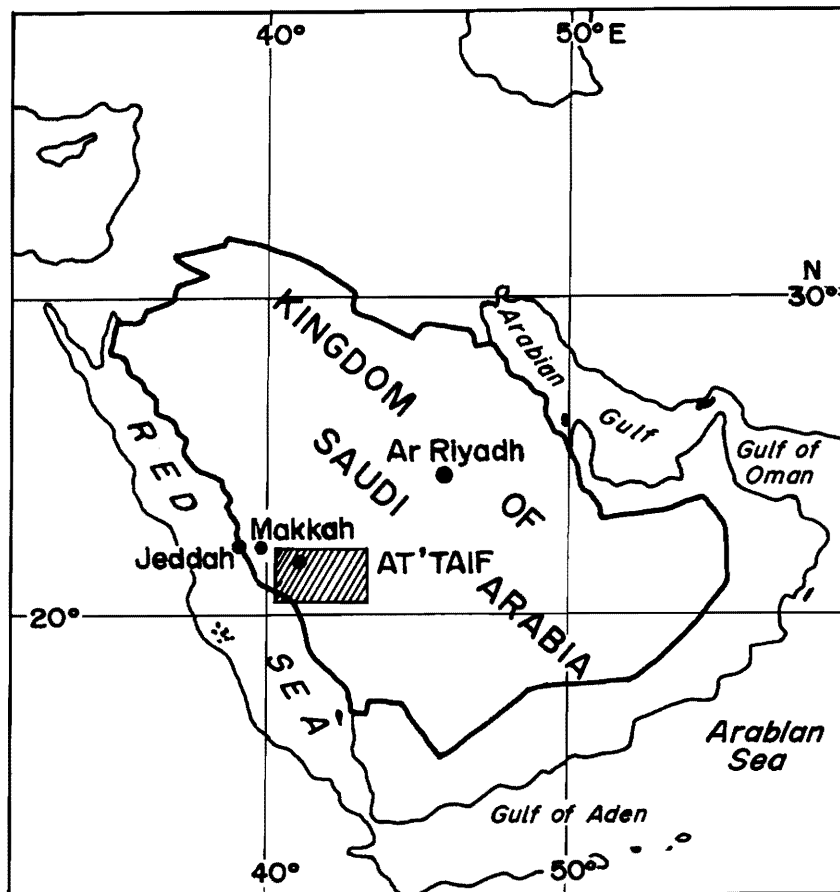


Figure 1. Location of Study Area.

1. At the northwestern feet of the escarpment:
  - (a) pre-tectonic granitoid rocks and
  - (b) late tectonic, calc-alkaline granitic rocks.
2. At the southeastern side of the escarpment:
  - (a) syntectonic granitic rocks and
  - (b) post-tectonic intrusive rocks.

The oldest radiometrically dated rocks in this assemblage are the syntectonic granites and granodiorites (containing many inclusions and xenoliths). These have mainly been derived from the granitization of schists and volcanic rocks. Age determinations of these rocks indicate a plutonic phase of equal age or slightly younger than the African Kilbaran Orogeny separated by an unconformity from these rocks are older andesites and diabases that can be found in the area around At-Taif. Similar rocks can also be found as intrusions within these granites.

Such Precambrian basement complexes have been subjected to two major orogenic cycles, the Hijaz and the Najd orogenies, with the Hijaz being the older and the more important. Consequently, strong folding, faulting, and even local overthrusting in meridional or north–northeast trending belts and lineaments predominate, indicating strong east–west compression.

The Najd orogeny relates to a younger period of mountain-building and cratonization. Its impact is expressed in a system of southeast–northwest trending left-lateral faults.

In a further stage of the tectonic history of the area, movements in connection with the spreading of the Red Sea Rift Zone became important. The tectonic movements in connection with this sea-floor spreading have not only provided the basaltic effusions but also remobilized the ancient joints and fractures [13–16].

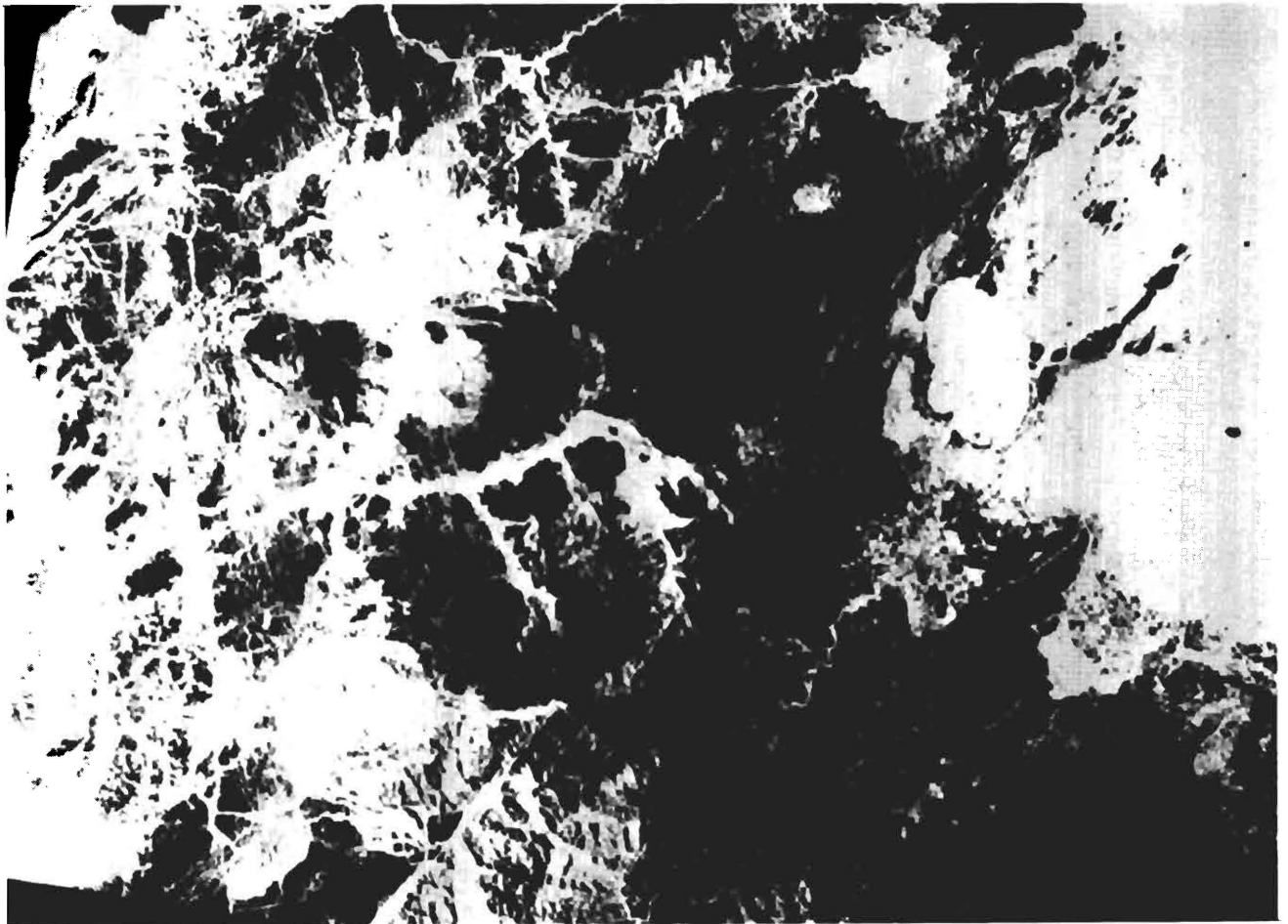


Figure 2a. Landsat TM Image of Study Area.

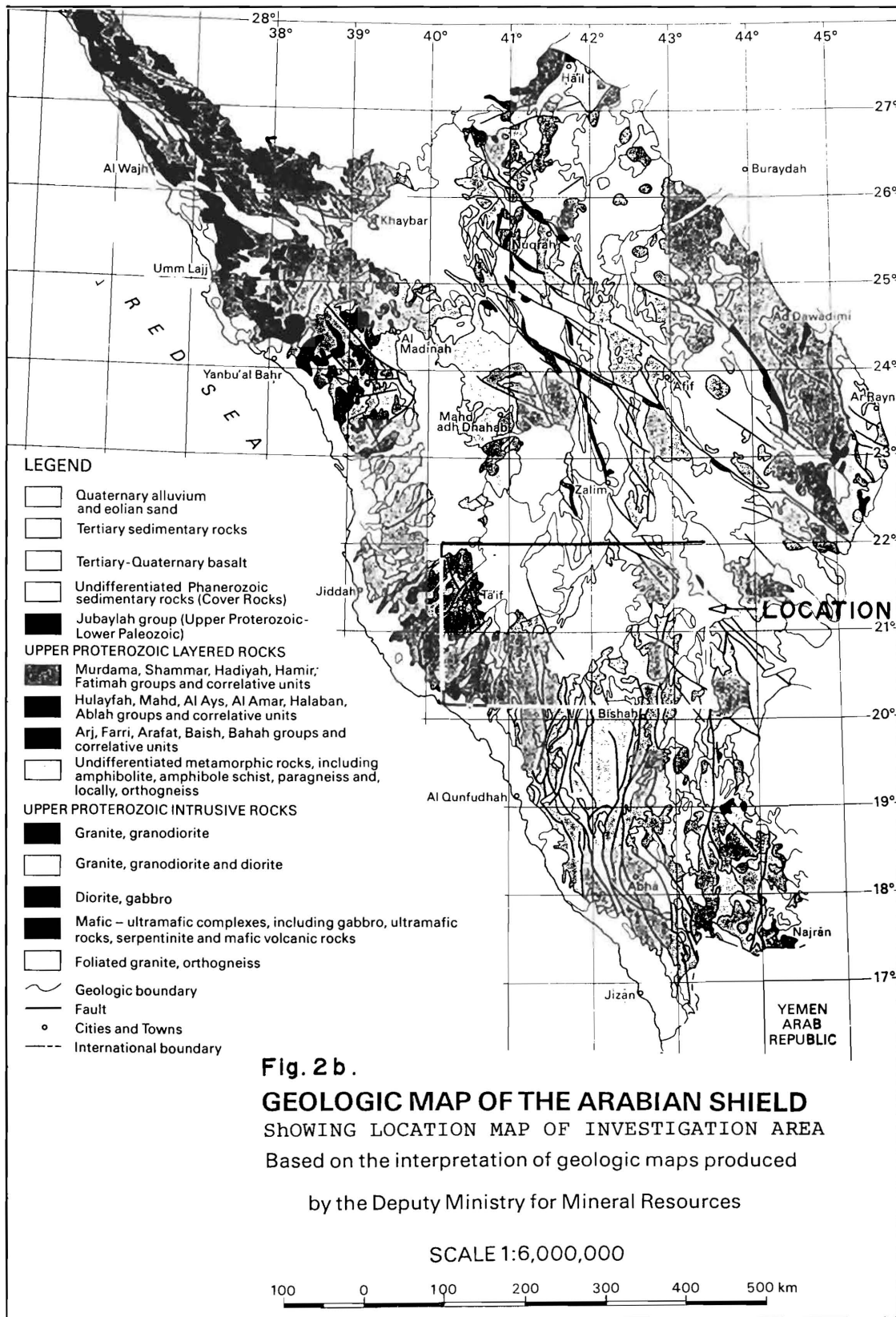


Figure 2b. Geologic Map of the Arabian Shield Showing Location Map of Investigation Area.

## 5. HYDROLOGIC INTERPRETATION

Mapping was carried out on transparent overlays, attached to the black and white "magenta" extract of the scale conformal lithographics. This ensures exact geometric accuracy between image and interpretation for the merging of the data layers in the final offset printing process. As the spectral information is more easily perceived, it is better for a differentiation. Color printing proofs of the geologic processing were also treated as in the case of the black and white aerial photographs to gather three-dimensional information and define run-off direction and watersheds.

### 5.1. Drainage pattern mapping

The drainage pattern was mapped (Figure 3) according to the following criteria:

- (i) In areas with outcropping rocks, drainage lines are positioned in valley bottoms, which can be traced by the higher albedo of valley sediments or a different albedo of the sun-exposed *versus* the sun-opposite slope. Both in areas with less relief and in wider valleys, differences are not prominent. In such places, vegetation is the main factor for identification.
- (ii) In areas covered with loose sediments, wadis can be identified by the spectral properties under consideration of geographical relationships. In most cases, the sediments of the temporarily carrying wadis exhibit a higher albedo. This is caused by the alluvium, or by the salt encrustation deposited after evaporation of the occasional water flow in the wadis. Another good indicator here is the higher vegetation density, seaming the wadi beds.

### 5.2. Tectonic control

With the help of the remote sensing data, faults and fractures can be directly identified together with a large number of other lineaments [17, 12].

Faults and fractures identified by such data can also be controlled on the ground, whereas a lineament may only be perceivable on the specific data set. Independent of the ground resolutions, both observation altitude, and illumination angle can influence the capability to observe distinctive lineament changes. For example, a very distinct lineament, detected on satellite imagery may appear as a clear cut simple linear feature. However, by aerial photography, it may

show as a broad feature composed of smaller elements with varying angles, not necessarily following the principal macroscale direction [17].

Taking this into account, the only characteristics, associated with lineaments, are "natural" and "subsurface phenomena" omitting any genetic relations [18]. This means that the single element itself has no tectonic significance. A meaningful interpretation can only be achieved on the basis of a statistical method. This was conducted in this study using a personal computer with a special software for computing compass diagrams of the directional distribution of the digitized lineaments.

Consequently, linear elements identified as faults or fractures on the basis of a certain direct displacement or through secondary indicators (*e.g.* curving of drainage lines, morphologic effects, *etc.*) were verified during the field campaign and compiled in the geologic interpretation (Figure 4).

All other elements were mapped separately and subjected to the statistical process.

## 6. THE DRAINAGE PATTERN AND ITS RELATIONSHIP TO TECTONICS

The analysis of both the geologic and drainage pattern maps (scale 1:50 000) of the area (Figures 4 and 5 respectively) has indicated that the drainage system is tectonically controlled. The first order wadis generally follow contacts between different formations or the main fault lines, which mainly trend NNE – SSW in the western and central parts of the area, while trending mainly N–S further to the east.

Second order tributaries usually follow fault directions orthogonal or sub-orthogonal to the main fault lines. These are sometimes also used by the first order tributaries as well to meander between main trend lines in an attempt to find their way according to the principle of least resistance (Figures. 4, 5 *a-h*).

The investigation area was subdivided into the following meaningful different measurement areas (Figure 4) representing the following rock units [18]:

- (gp): Red to pink, nonmetamorphic alkali to peralkali granite, (of post-tectonic genesis).
- (gg): Granite to granitic gneiss of gray color with many inclusions and xenoliths largely derived from granitization of schists and volcanic rocks. The basement genesis is believed to

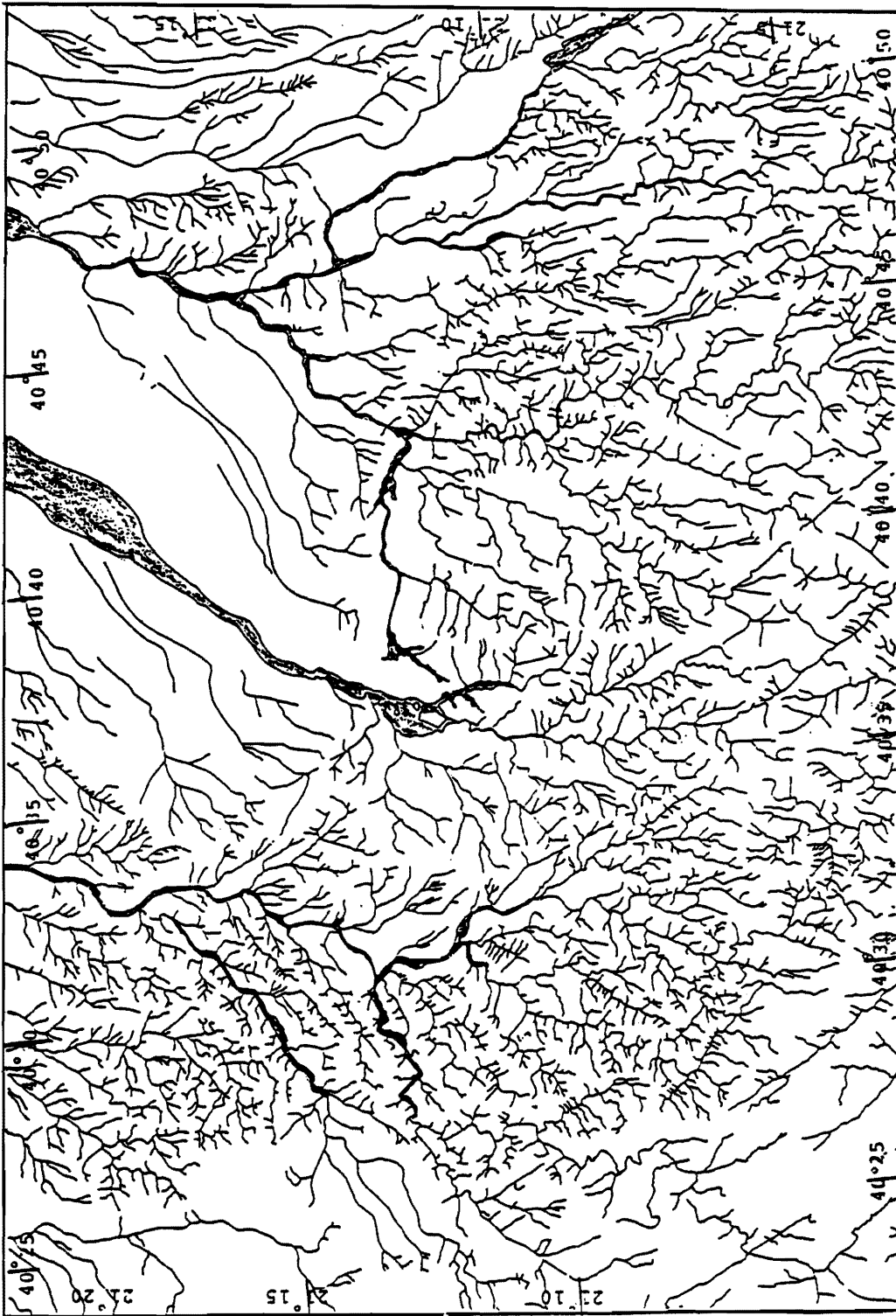


Figure 3. Drainage Pattern Map of Taif Area.

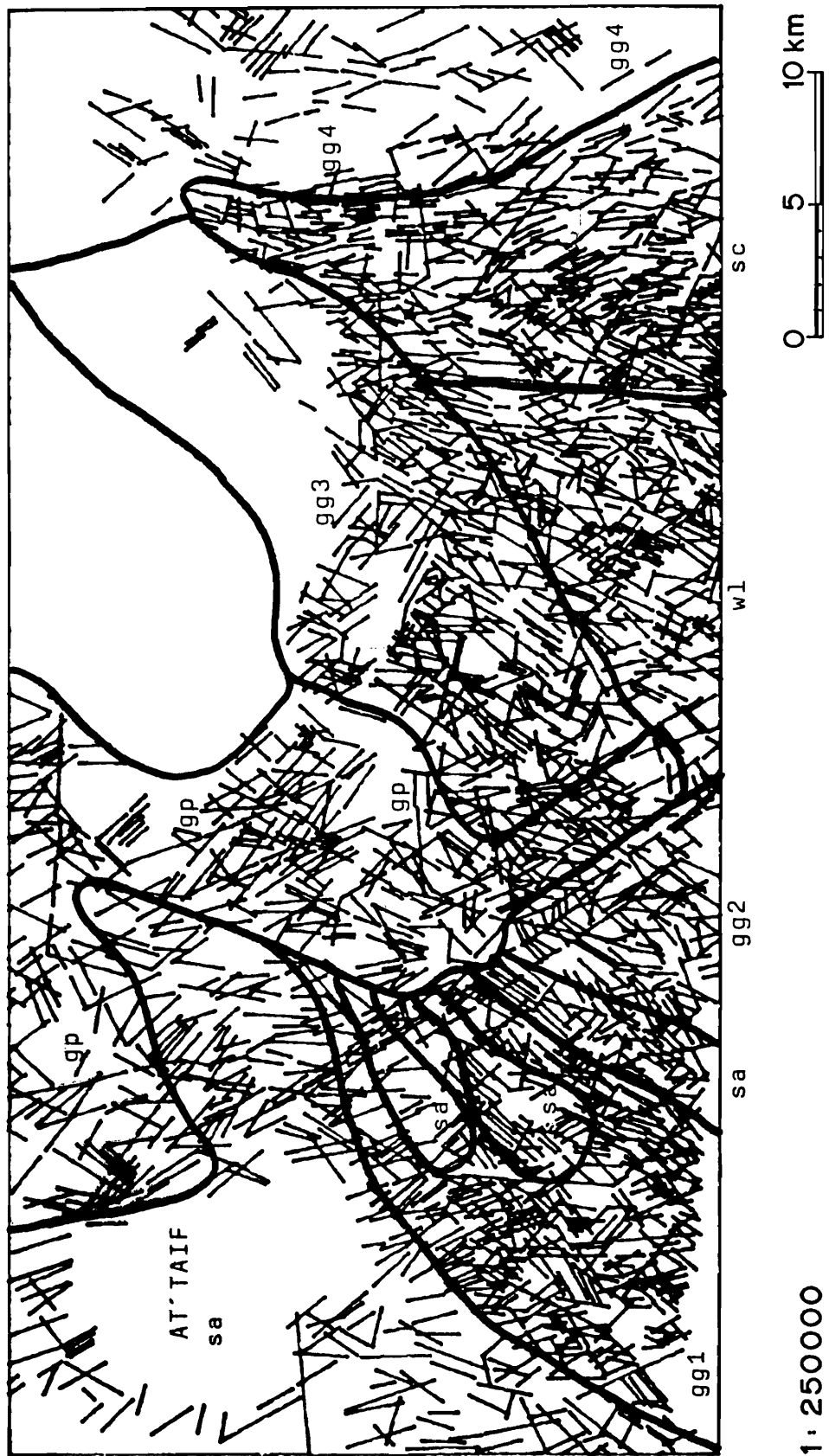


Figure 4. Area of Statistical Evaluation.

represent the oldest Precambrian rocks in this region.

- (gqd): Diorite and granodiorite, often gneissic, including sometimes sheared and metamorphosed quartz-diorite and adamellite, often with megmatitic, xenolithic metamorphic rocks, usually containing amphibolites.
- (sc): Sericite- and chlorite-schist (derived largely from sediments), quartzitic conglomerates, less jaspilite, arkose-quartzites, graphitic schists and marbles, locally amphibolitized.
- (sa): Amphibolitic schists, largely derived from greenstones and keratophyres, with sericitized schists, little portions of gray, pink, and light brown marbles and quartzites. Largely interspersed with granite plugs.

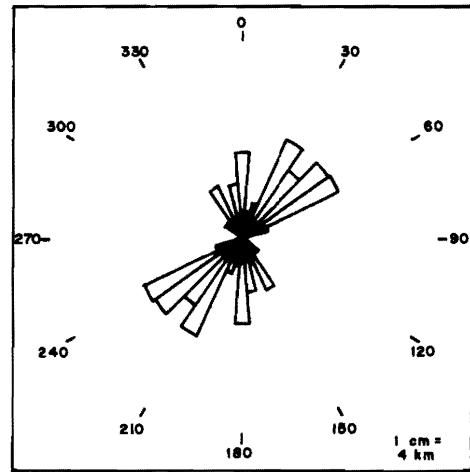


Figure 5c. Lineaments of Thematic Mapper Data 1 : 50 000 / Unit GG Part 2.

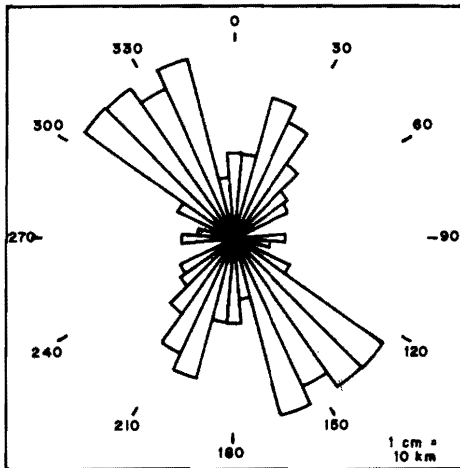


Figure 5a. Lineaments of Thematic Mapper Data 1 : 50 000 / Unit GP Part 1.

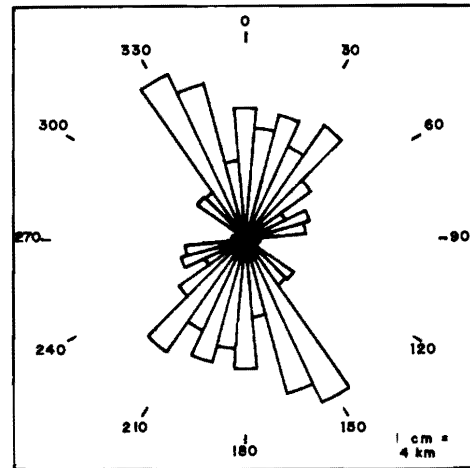


Figure 5d. Lineaments of Thematic Mapper Data 1 : 50 000 / Unit GG Part 3.

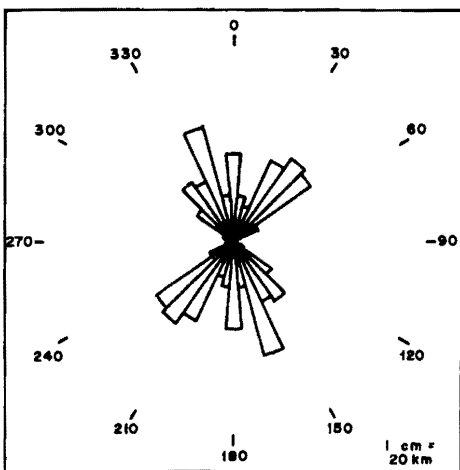


Figure 5b. Lineaments of Thematic Mapper Data 1 : 50 000 / Unit GG Part 1.

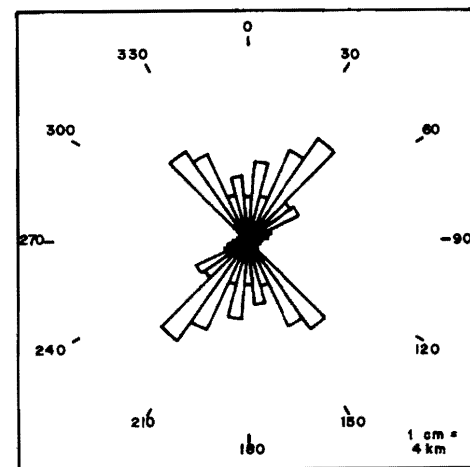


Figure 5e. Lineaments of Thematic Mapper Data 1 : 50 000 / Unit WL.

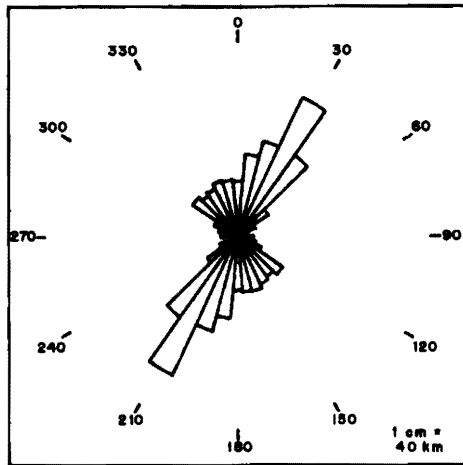


Figure 5f. Lineaments of Thematic Mapper Data  
1 : 50 000 / Unit GG Part 4.

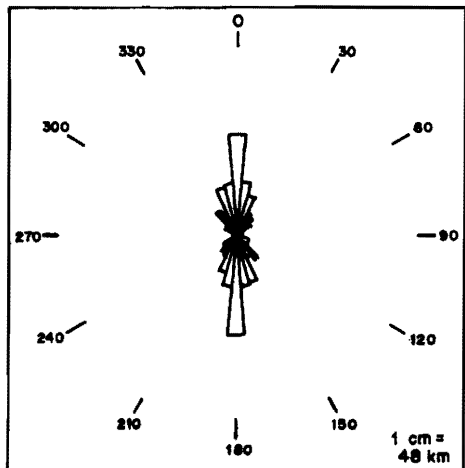


Figure 5g. Lineaments of Thematic Mapper Data  
1 : 50 000 / Unit SC.

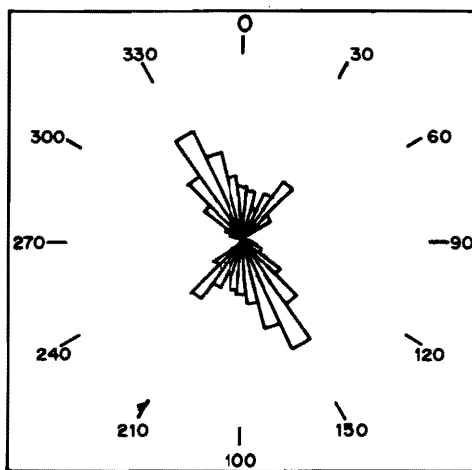


Figure 5h. Lineaments of Thematic Mapper Data  
1 : 50 000 / Unit SA Total (1-4).

(wl): Wadi Lith complex, includes metadiorites, metagabbros, and amphibolites and a subordinate amount of schists and quartzite, often gneissic.

Considering the directional dependence of the length of the mapped lineaments with regard to tectonic phenomena, the model of Sander [19] was used for the interpretation of the compass diagrams. According to this model, when rocks are subjected to stress, fractures as presented in Figures 6 and 7 occur. The direction of the tectonic transport or stress axis along  $a$  and  $b$  is the direction of the deformation axis (Figure 6). The planes  $ab$ ,  $ac$ , and  $bc$  are the main planes of normal stress and each one is oriented parallel to the two axes of the coordinate system. Opposite to this, each one of the pairwise occurring shear fractures (Figure 7) is parallel to only one axis of the coordinate system. Considering this as well as the overall geologic/tectonic situation, the following interpretation can be suggested.

Figure 5a shows a distinct maximum around 1500, which is also shown in Figures 5b and 5d. However, in the latter Figures, this maximum is accompanied by a further peak at an angle varying between 60° and 70°. The position of this peak in the compass diagrams rotates clockwise from 20° to 30° in Figure 5a via 30° to 50° in 5b, then 30° to 60° (emphasis 50° to 60°) in Figure 5d, back again to 30° to 40° in 5e and 5f, with an opening of the angle in the latter Figures.

According to the overall tectonic history of the region, the maxima ranging between 30° and 60° may represent  $bc$  fractures of a direction around northeast-southwest with varying compressing forces, which can be correlated to the Hijaz orogeny. The corresponding maximum which has shifted counterclockwise by 50° to 70° in the diagrams may be identified with unbranched  $hkO$  shear joints of that phase. The reason

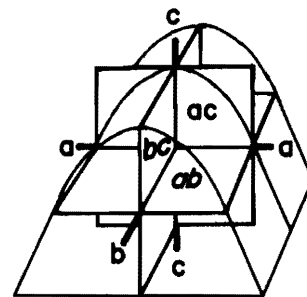


Figure 6. Structure Coordinates,  $a$ ,  $b$ ,  $c$ , and the Correlating Fracture Planes.

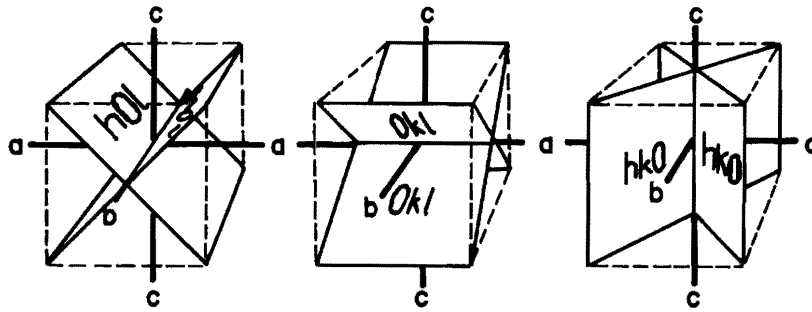


Figure 7. Structure Coordinates  $a, b, c$ , with their Pairwise Shear Planes.

for detecting only dextral shear joints in the satellite image is that these joints have been reactivated by the Red Sea rifting, starting in Paleogene time, so that along these lines erosional forces could become effective and define the drainage lines. Sinistral  $hkO$  joints may also be present but are not visible on macroscale, as they have no geometric relationship to the rifting process. This theory is testified by the fact that the higher distance is between the geomorphologically very prominent escarpment west of At'Taif, (which is related to rifting) and the measurement area, where the most ancient  $bc$  fractures occur to the debit of  $hkO$  directions. In the extreme cases, practically only  $hkO$  (Figure 5a, unit gp) and  $bc$  directions (Figure 5h, unit gg4) are represented.

Figure 5g differs distinctly from the other figures by its north–south directed maximum. As the figure represents lineaments presumably reflect schistosity rather than structural lines.

The  $30^\circ$  and  $70^\circ$  maxima correlate with the direction of the main wadis, as presented in the maps, and thus support their interpretation with  $ab$  fractures of an orthogonally compressing force. The most extensive fractures during orogenic folding occur in  $ab$  directions, and these are the most easily eroded fractures.

## 7. CONCLUSION

The drainage pattern of the area around At'Taif was analyzed in a synergistic approach. This was carried out by taking into account geology and tectonics, as revealed on LANDSAT-Thematic Mapper satellite imagery, and confirmed in the field.

The investigations show that the drainage pattern in the area is largely controlled by structures of the late Cryptozoic Hijaz orogeny, which was accompanied by

compression from different directions, and was later reactivated by the Red Sea rifting during the Paleogene.

## ACKNOWLEDGEMENT

I am grateful to Dr. Alwash and Dr. Zakir of the Faculty of Earth Sciences for their cooperation in preparing Figure 2b. I am also indebted to King Abdulaziz University for providing financial support that enabled this research to be undertaken.

## REFERENCES

- [1] C. W. Thornthwaite, "Problem in the Classification of Climates", *Geographical Review*, **33** (1943) p. 233.
- [2] C. W. Thornthwaite, "An Approach Toward a Rational Classification of Climate", *Geographical Review*, **38** (1948), p. 55.
- [3] D. J. Burdon and G. Otkun, "Hydrogeological Control of Development in Saudi Arabia", *XXIII International Geological Congress*, **12** (1986), p. 75.
- [4] Ministry of Planning, *The Fourth Development Plan*. Riyadh: Ministry of Planning, Kingdom of Saudi Arabia, 1405–1410 H./1985–1990, p. 161 (in Arabic).
- [5] Ministry of Planning, *The Fifth Development Plan*. Riyadh: Ministry of Planning, Kingdom of Saudi Arabia, 1410–1415 H./1990–1995, pp. 105–107 and 217–225 (in Arabic).
- [6] Ministry of Planning, *The Third Development Plan*. Riyadh: Ministry of Planning, Kingdom of Saudi Arabia, 1400–1405 H./1980–1985, p. 111 (in Arabic).
- [7] G. Otkun, *Some Aspects of Groundwater Distribution and Exploitation in Saudi Arabia*. Riyadh: Ministry of Agriculture and Water, Kingdom of Saudi Arabia, 1972 (unpublished report).
- [8] A. F. H. Goetz and L. C. Brown, "Geologic Remote Sensing", *Science*, **211** (1981), p. 781.
- [9] H. C. Andrews, *Introduction to Mathematical Techniques in Pattern Recognition*. New York: Wiley

- Interscience, 1972; Gillespie, in *Remote Sensing in Geology*. eds. B. S. Siegal and A. Gillespie. New York: Wiley 1980, ch. 6.
- [10] A. Y. Bokhari, "Hydrological Investigations in the Western Al Madinah Quadrangle, Kingdom of Saudi Arabia, on the Basis of Landsat Thematic Mapper Data", *Berliner Geowissenschaftliche Abhandlungen*, **C10**, (1988), p. 113.
- [11] A. Y. Bokhari, "Hydrological Investigations East of Al Madinah/Saudi Arabia, on the Basis of Landsat Thematic Mapper Data", *Berliner Geowissenschaftliche Abhandlungen*, **C12**, (1991), p. 97.
- [12] T. M. Lillesand and R. W. Kiefer, *Remote Sensing and Image Interpretation*. New York: Wiley, 1979, p. 612.
- [13] G. F. Brown, *Tectonic Map of the Arabian Peninsula*. Jeddah: Ministry of Petroleum and Mineral Resources, Kingdom of Saudi Arabia, 1983.
- [14] G. F. Brown and R. O. Jackson, "The Arabian Shield", *XXI International Geologic Congress*, **9**, (1960) p. 69.
- [15] G. F. Brown and R. O. Jackson, "Eastern Margin of the Red Sea and the Coastal Structure in Saudi Arabia", *Philosophical Transactions of the Royal Society, London*, **A 267** (1970), p. 75.
- [16] R. O. Jackson, *A Preliminary Lithofacies Map of the Saudi Arabian Shield*. Jeddah: Ministry of Petroleum and Mineral Resources, Kingdom of Saudi Arabia, 1983.
- [17] G. Henderson, "Air-Photo Lineaments in Mpanda Area, Western Province Tanganika", *American Association of Petroleum Geological Bulletin*, **44** (1960) p. 53-71.
- [18] D. W. O'Leary, J. D. Friedman, H. A. Pohn, "Lineament, Linear, Lineation, Some Proposed New Standards for Old Terms", *Geological Society of American Bulletin*, **87** (1976) p. 1463.
- [19] B. Sander, *Einführung in die Gefügekunde der geologischen Körper*, Vienna: Springer, **I** (1948), p. 215.

**Paper Received 18 March 1992; Revised 23 May 1992.**